Geo-Marine Letters (1998) 18: 49–57

P. Ciavola · N. Dias · Ó. Ferreira
R. Taborda · J. M. A. Dias

Fluorescent sands for measurements of longshore transport rates: a case study from Praia de Faro in southern Portugal

Received: 16 May 1997 / Revision received: 20 November 1997

Abstract A field experiment was carried out on a mesotidal reflective beach to relate longshore sand transport rates to wave measurements in medium-energy conditions ($H_{rms} = 0.6$ m; $T_m = 6.5$ sec; $\alpha = 20°$). Dispersion of fluorescent sand tracers was analyzed using the spatial integration method (SIM). The measured sand transport rate was three times larger than the prediction computed using the longshore wave power approach, while the K factor was determined empirically as 2.32. The study concluded that there is a need to calibrate bulk longshore transport predictors before applying them to steep gradient slopes under plunging waves.

Introduction

Historically, measurements of longshore sand transport rates were first undertaken using deposition rates in the lee of coastal structures such as groins, breakwaters, and jetties (Komar 1988). This methodology has two main disadvantages, namely, the long time required to obtain significant information (from months to years) and the local effects on waves and currents caused by the structure itself (e.g., wave diffraction). It became clear that it was necessary to develop a technique able to measure transport rates under different spatial and temporal scales. Recent research has produced new technologies for measurements at a micro scale such as optical back scatter (OBS) sensors (Downing et al. 1981) or acoustical back scatter (ABS) sensors (e.g., Vincent et al. 1991). However, besides the use of sediment traps for meso-scale measurements (Allen 1985; Kraus 1987) at a larger scale sand tracers have been the most widely used methodology (Allen 1988).

One of the first experiments using tracers dates back to the beginning of the present century (Richardson 1902), but as Kidson and Carr pointed out (1971) it was only in the 1950s when serious development of the technique took place, rendering it popular with many investigators in the United Kingdom and Japan, particularly using radioactive isotopes for tagging. Towards the end of the decade, a group of investigators in the former Soviet Union started to use sand marked with fluorescent paint (Zenkovitch 1960), and in the following years, investigators concentrated on selecting the best types of paints (Yasso 1966) and optimizing marking procedures (Ingle 1966). The usage of fluorescent sand is simple, marking can be done easily and rapidly, there is no impact on health and the environment, different colors can be used to tag various grain fractions to study differential transport, and the sensitivity of the technique is at least one in a million (Ingle 1966). The method must fulfill some basic assumptions: the marked sands should have an hydraulic behavior comparable to the unmarked ones, advection of the tracers should be prevalent over diffusion and dispersion, and the transport system must be in equilibrium (Madsen 1987).

The tracer technique first was applied on Portuguese beaches in the 1960s by Abecasis et al. (1962) who used fluorescent sand on the coast of northern Portugal. In that case, the authors used sand marked with fluorescent paint and radioisotopes at the same time, obtaining better results with the second method, since natural luminescence from the grains caused confusion with the first one. The technique became of interest to Portuguese researchers

P. Ciavola (✉)
Dipartimento di Scienze Geologiche e Paleontologiche, Università di Ferrara, Corso Ercole I d-Este, 32 Ferrara, 44100, Italy

N. Dias · Ó Ferreira · J. M. A. Dias
Unidade de Ciências e Tecnologias dos Recursos Aquáticos, Universidade do Algarve, Campus de Gambelas, 8000 Faro, Portugal

R. Taborda
Departamento de Geologia, Universidade de Lisboa, Cidade Universitária, Faculdade de Ciências, Bloco C2, 5° Piso, Campo Grande, 1700 Lisboa, Portugal

once again in the 1990s, with the development of the *Luminóferos na Areia* (LUAR) experiments undertaken by the DISEPLA research group (Taborda et al. 1994; Ciavola et al. 1997a). These experiments introduced several improvements to the methodology, in particular regarding the automatic detection of marked sand grains on the beach (Pinto et al. 1994) and the study of tracer dispersal along three dimensions (Ciavola et al. 1997a).

This paper describes the application of these recent developments in sand tracing research to Praia de Faro, a meso-tidal beach in the Algarve barrier-island system. The experiment (LUAR-Faro 1996) took place on 6–7 March 1996 and its main aim was to produce a new data set of longshore transport measured on a steep beach in a medium energy environment. Although recent experiments carried out in Portugal (Taborda et al. 1994; Ciavola et al. 1997a) partially fulfilled the lack of data from steep-gradient beaches, the information produced was either from high- or low-energy settings.

Study site and oceanographic setting

The study area is located in the Algarve region of southern Portugal, in the central part of the Ancão spit (Fig. 1), the westernmost unit of the Ria Formosa lagoon. The lagoon is separated from the open sea by a barrier-island system that extends 55 km. The lagoon communicates with the sea through a network of branched creeks, channels, and six inlets, two of which are stabilized by concrete piers. Tides have a semidiurnal regime and amplitude varies from a maximum of 3.5 m at spring tides to a minimum of 0.5 m at neap tides (Andrade 1990).

The Ancão spit has a length of approximately 10 km that changes temporarily with the migration of the Ancão tidal inlet (Pilkey et al. 1989). As such, it is considered one of the most fragile of the barrier islands and spits of the system (Bettencourt 1994). The spit has an orientation of N 55°W and is between 50 and 250 m wide, with a trend of migration towards the southeast. There is a single dune ridge, except in the central part of the spit (Praia de Faro, the study site) and overwashes are frequent (Pilkey et al. 1989; Tomé Martins et al. 1996).

Average wind speeds in the area rarely exceed 60 km h^{-1}. Although dominant (both in frequency and speed) winds blow from the southwest, high-energy events sometimes occur from the northeast and from the southeast (Instituto Nacional de Meteorologia e Geofísica 1979 and 1981 in Bettencourt 1994). Pessanha and Pires (1981) indicated that the typical average values of significant wave height and period in the offshore region of the Algarve are 0.9 m and 5.0 s, which is in agreement with recent data measured by the Instituto Hidrográfico and the Laboratório Nacional de Engenharia Civil (1994) offshore the Faro tidal inlet (Cabo S. Maria). Pires (1985) divided all observations into two main categories, southwestern and southeastern (*levante*) quadrants. The southwestern quadrant includes waves generated by meteorological events on the western Portuguese coast, particularly storms with westerly winds. These are high-energy events able to generate waves in the Algarve region with heights of 2–3 m and periods of 7–8 s. High-energy events belonging to the *levante* quadrant are not frequent during the year, but are normally related to strong winds blowing from the southeast in the Gibraltar Strait. The wave spectrum from this direction is normally narrow, with low directional spreading, and average wave height and period are approximately 1.2 m and 4.9 s (IH/LNEC 1994). According to the Instituto Hidrográfico and the Laboratório Nacional de Engenharia Civil (1994), about 51.5% of waves measured by the wave-rider buoy offshore Cabo de S. Maria (Fig. 1) come from the W, 16.3% come from the SW, 2.1% from the S, 25% from the SE, and 4.2% from the E. Storms from the southwest have short duration, normally between two and four days, and occur in the winter season, with wave heights rarely exceeding 4.0 m and occasionally reaching 6.0 m (Pires 1985). South-easterly storms are of longer duration, at times over a week, and wave heights rarely exceeding 4.0 m (Andrade 1990). Generally these waves approach the coast at large angles, generating strong longshore currents and large longshore transport rates, causing erosion along the barrier islands, with formation of wave-cut beach scarps (Tomé Martins et al. 1996).

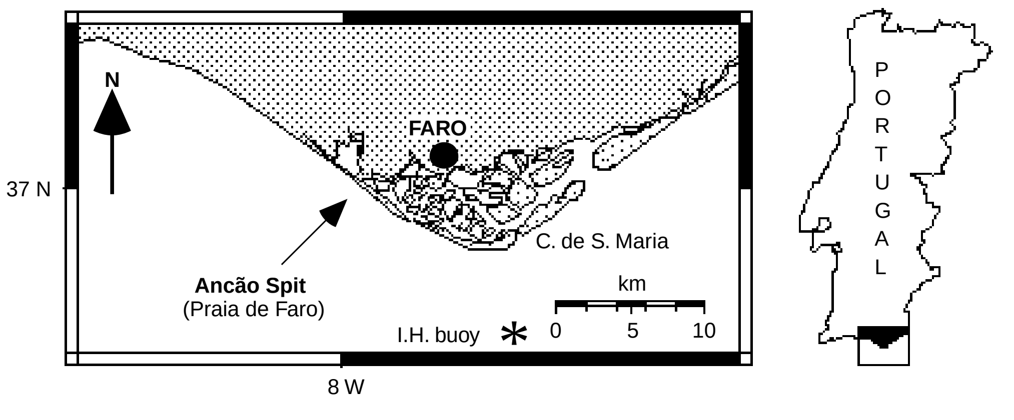

Fig. 1 Location of the study area and approximate position of the Instituto Hidrográfico wave-rider buoy

The beaches of the Ria Formosa system mainly consist of quartzitic sands with a smaller fraction of small pebbles and biogenic (shell fragments) material (Andrade 1990). Mean grain size shows variations longshore and from one island to the other one, being generally medium sand (Pilkey et al. 1989). The predominant southwesterly wave motion produces a net longshore drift eastwards, but there is no agreement between authors on the magnitude of the transport. Published estimations for the Ancão spit range from $6 \times 10^3\,\mathrm{m}^3\,\mathrm{yr}^{-1}$ (Andrade 1990) to $3 \times 10^5\,\mathrm{m}^3\,\mathrm{yr}^{-1}$ (CONSULMAR in Bettencourt 1994). Previous studies believe that the source areas for the sands are the continental shelf and the erosion of the cliffs near Quarteira (Dias 1986; Bettencourt 1994; Andrade, 1990).

Methodology

Wave visual observations

During the high tide of 6 March 1996, direct observations of wave height and period and measurements of angle of approach at wave breaking were carried out every hour to provide a comparison with values measured with an array of pressure transducers. Mean wave height at breaking point was recorded by two independent observers that estimated heights for a 10-min interval and then averaged the values. Mean wave period was computed by dividing the observation time interval (600 s) by the number of counted waves. The angle of wave approach at breaking point was measured applying the methodology of Chandramohan et al. (1994), based on the formula:

$$\sin \alpha_b = (3.54 \Delta T \sqrt{H_b})(S + W) \tag{1}$$

where (α_b) is the angle of approach at the breaking point, H_b the wave height at breaking, ΔT the time used by a wave crest to travel from a reference point along a line orthogonal to the beach to a second point along a line at 45 degrees with origin to the observer, S the distance between the observer and the mean water mark, and W the distance between the mean water mark and the breaker.

Wave and wind measurements

Three Keller PA-46 pressure transducers were deployed in a triangular array arranged around a metal frame, located on the lower beach face, just above low tide level. The pressure transducers were connected through an analog-to-digital converter card to an IBM-compatible PC, which sampled continuously the signal at a frequency of 5 Hz. Voltage readings were then converted into pressure values using calibration equations obtained from laboratory tests undertaken before deployment. Spectral analysis of the signal was carried out using routines of the digital signal processing toolbox, part of the MATLAB software package. Wind conditions during the experiment were recorded every 30 min using a compass and an anemometer.

Usage of tracers in the field

During the week before the experiment (1 March 1996), a composite sand sample of 125 kg was collected at Faro Beach. The composite sample was obtained by mixing three samples collected, respectively, on the lower, mid, and upper beach face during low tide. The sand was washed with freshwater to remove salt and dried in the open air, spreading it over a flat surface to facilitate the process. It was subsequently marked following methodologies and recommendations of previous authors (e.g. Ingle 1966; Yasso 1966; Taborda et al. 1994; Ciavola et al. 1997a). The tracer was prepared with a fluorescent orange paint, produced by Atomlac Industrie (Glycero Orange Floo), using a paint (liters)/sand (kg) ratio of 0.05 after adding 20% thinner to the paint. The sand was then dried in the open air, trying to minimize aggregate formation, and later sieved using a 2-mm mesh. A subsample (100 g) of the marked population was collected to compare grain size distributions before and after tagging. Mean grain size, sorting, standard deviation, and kurtosis were determined using the method of moments.

On the morning of 6 March 1996, a 2.1×1.1-m rectangular trench was dug on the beach face at low tide to a depth of 0.03 m; it was located at 19 m seaward of the berm. The tagged sand was put into the trench after lubricating it with a mixture of water and liquid detergent to avoid grain aggregation and transport as floating sand.

During the following low tide, the distance of maximum tracer transport was assessed in the field carrying out spot checks, moving away from the injection point in the direction of longshore drift, using a UV lamp connected to a portable power supply, mounted on a 4-wheel-drive all-terrain vehicle (ATV). The size and mesh of the sampling grid was chosen in relation to the maximum distance of tracer advection, that was 1900 m away from the injection point (Fig. 2). Four teams of four samplers ran 27 shore-normal profiles with longshore spacing of 50 m for the first kilometer away from the injection point and 100 m spacing up to the last transect. Shore-normal spacing between samples along a profile was 10 m, with up to six samples collected in a single transect between the berm and the area of breakers at low tide. At each sampling station a small core, 50 cm long and 5 cm in diameter, was collected using PVC pipes. The pipes had been cut lengthwise into two halves that were held together by hand and pushed into the sand. After retrieval, each shallow core was opened and divided into 5-cm sections. Sampling of the seabed in the breaker zone at low tide was undertaken by divers using small plastic cases. Counting of tracer distribution at the surface around the points where cores were collected was undertaken using a predefined area of

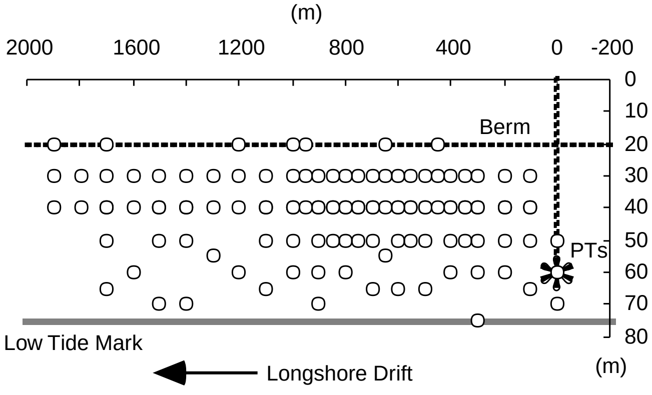

Fig. 2 Sampling grid of shallow beach cores. The star in the diagram identifies the position of the pressure transducers (PTs)

30 cm × 30 cm and a UV lamp inside a dark box. It was intended to carry out a second sampling at the following low tide on 7 March 1996, but early inspection revealed that the concentration of the tracer had become too low to be significant, meaning that more tracer should have been used initially. Beach samples were collected along a transect including the injection point, and grain size analyses were undertaken to determine differences between the marked sands and the natural beach sediment. Morphological profiles were measured every 50 m away from the injection point, for a total of 11 profiles, to provide information on erosion and accretion events that could have caused burial of the tracer.

Laboratory analyses of tracers

Each subsample was wet sieved with freshwater in the laboratory using a 63 µm mesh sieve, then put on a Petri dish, dried in an oven at 60°C, and weighted using a balance with a precision of 0.1 g. After sieving, the number of fluorescent grains was counted under a UV lamp. The results from the samples collected at Praia de Faro were analyzed using the spatial integration method (SIM) (Madsen 1987), a method that has been widely used in previous studies (e.g., Komar and Inman 1970; Kraus et al. 1982; Taborda et al. 1994; Ciavola et al. 1997a), because its Lagrangian approach allows monitoring of tracer movement both in space and time. Other advantages of the SIM over other types of integration (e.g., time integrated method, continuous injection method) is that the velocity of transport is calculated referring it to the centroid of the tracer cloud and that it is possible to calculate with confidence a recovery rate (Madsen 1987). The mass of recovered tracer in each 5-cm layer was calculated using the following formula:

$$\text{Mass of recovered tracer sand} = A\,h\,D\,\rho_s\,(1-p) \qquad (2)$$

where A is the area of which the core is representative (obtained by analysis of the sampling grid), h the thickness of the sample (5 cm), D the dilution of the tracer (mass of counted fluorescent grains per total mass of the sample), ρ_s the sand density (2650 kg/m^3), and p the sand porosity (0.4). Summing all masses obtained from the samples makes it possible to calculate the percentage of tracer recovery (total mass recovered per total mass injected).

The longshore position of the tracer-cloud centroid in each 5-cm layer was obtained by applying the relationship:

$$Y = \frac{\Sigma M_i d_i}{\Sigma M_i} \qquad (3)$$

where M_i is the mass of tracer recovered at a distance d_i from the injection point, and i is the number of samples. The velocity of the centroid is obtained dividing Y by the time between two successive low tides (45×10^3 s). Such velocity was calculated for each 5 cm layer weighting it against the mass of tracer recovered in each layer.

In order to calculate the volume of transported sand, it is necessary to calculate the mixing depth that is considered equivalent to the thickness of the moving layer. Within this layer, grains are subjected to vertical and lateral movements caused by direct wave action (e.g., swash and backswash) and by the superimposed longshore current (Kraus 1985). There are different methods in the literature for determining in the field the thickness of the layer, namely to dig one or more control holes filled with marked sand (King 1951; Komar and Inman 1970; Taborda et al. 1994; Ciavola et al. 1997b) or refer changes in beach height to reference rods (Greenwood and Hale 1980). For the study at Praia de Faro, the mixing depth was identified as the interval within beach cores where 80% of the tracer was recovered (Kraus et al. 1982; Kraus 1985; Ciavola et al. 1997b).

Results

The visually observed mean breaking wave height H_{bm} and period T_{bm} were 0.8 m and 9 s, respectively. These values are comparable with those of significant wave height and peak period obtained by spectral analysis (Table 1). Waves were coming from the *levante* quadrant (SE), with an approach angle at breaking of 20°, plunging directly onto the beach face. The difference between deep-water wave measurements (Table 1) from the Instituto Hidrográfico wave-rider buoy offshore Cabo S. Maria and the measurements at Praia de Faro (Table 1) is probably due to the triangular shape of the barrier-island system (Fig. 1), which creates a shadow area westwards of the Cabo de S. Maria, so that southeasterly waves arrive along the Ancão spit after undergoing considerable near-shore wave refraction, diffraction, and energy dissipation. Average recorded wind directions and speed were 88°N and 4.2 m/s, respectively.

The beach showed accretion during the high tide of 6 March (PM) on the order of 0.2–0.3 m (Fig. 3) and

Table 1 Comparison between wave parameters measured at Faro Beach during the experiment and offshore wave conditions

Location	Significant wave height (m) [H_s]	Root mean squared wave height (m) [H_{rms}]	Zero-up crossing period (s) [T_z]	Average period (s) [T_m]	Peak period (s) [T_p]
Breaking Point (Faro Beach)	0.8	0.6	5.4	6.5	10.0
Offshore (Cabo S. Maria)[a]	1.4 (low)[b] 1.9 (high)[c]	Not supplied	Not supplied	6.0	8.0

[a] Data measured by the Instituto Hidrográfico wave-rider buoy at a water depth of about 103 m
[b] Computed for low frequency waves ($T > 8$ s)
[c] Computed for high frequency waves ($T < 8$ s)

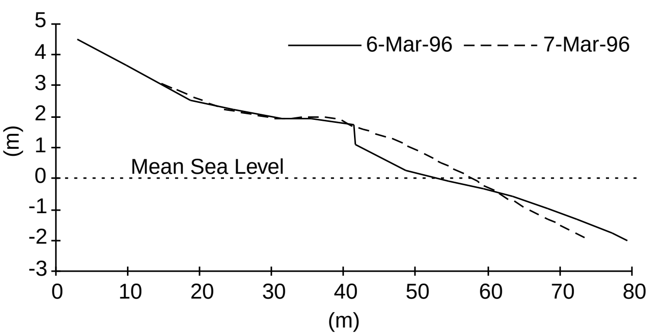

Fig. 3 Changes in beach profile measured during the experiment

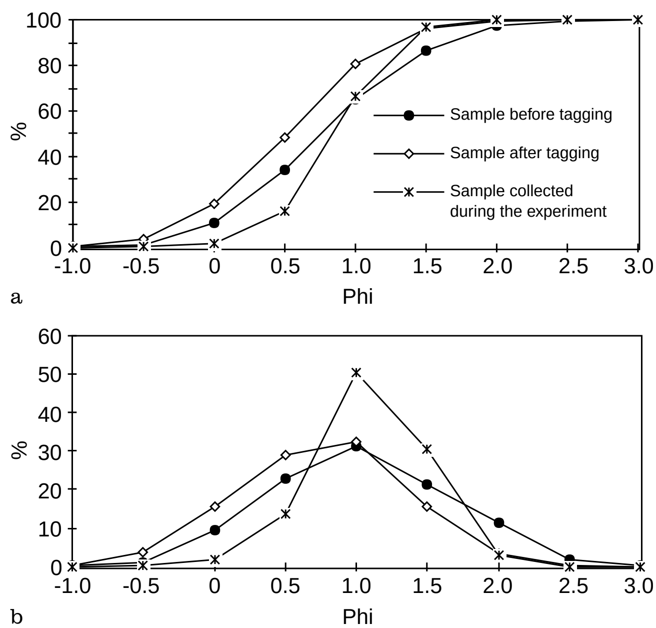

Fig. 4 **a**: Comparison between absolute frequency curves of grain size populations; **b**: comparison between cumulative frequency curves of grain size populations. Grain size is expressed in phi units [phi $= -\log_2$(mm)]

erosion on the lower part of the profile during the high tide of 7 March AM (Fig. 3), while the average beach slope (tanβ) measured at the beginning and at the end of the experiment varied between 0.08 and 0.11 (Fig. 4). The latter parameter, together with the observed mean wave height H_{rms} and period T_m can be used to calculate the surf scaling parameter ε of Guza and Inman (1975):

$$\varepsilon = \frac{(a\omega^2)}{g\tan^2\beta} \tag{4}$$

where tanβ is the beach slope, g the gravitational constant, a the wave amplitude $H_{rms}/2$, and ω is wave radian frequency ($2\pi/T_m$). The obtained value of 4.47 describes the beach morphodynamics as intermediate at the beginning of the experiment (profile of 6 March in Fig. 3), while the value of 2.36 indicates a reflective behavior by the end of the experiment (profile of 7 March in Fig. 3).

Mean grain size of the beach sand before tagging was 0.58 mm, it became slightly coarser after painting (0.70), despite taking care to minimize aggregate formation. However, comparison of absolute and cumulative frequency curves (Figs. 4a, b) shows that the modal class is similar throughout the three populations.

During the experiment, tracer was driven westward by southeasterly waves up to 1900 m away from the injection point. Beach cores generally reached a depth of 30 cm below surface. Some of them contained anomalous tracer concentrations below 25 cm, probably due to local beach accretion and were eliminated as suggested by Kraus (1985). Samplers in the breaker zone at low tide only collected sand from the surface layer down to a maximum depth of 5 cm. Concentrations of marked grains for each sampled depth in the cores are presented in Fig. 5. Percentage of tracer recovery was about 90% of the injected mass.

The average cross-shore profile of sand mixing depth is represented in Fig. 6. The thickness decreases towards the top of the berm where there is minor sediment activation, giving an average mixing depth of about 23 cm. From Fig. 6, the cross-shore area corresponding to the active sand layer is 9.25 m^2. The average velocity of the centroid was calculated as 0.015 ms^{-1}, that multiplied by the area of the active sand layer gave a volume of 0.140 m^3 s^{-1} (12×10^3 m^3 day^{-1}).

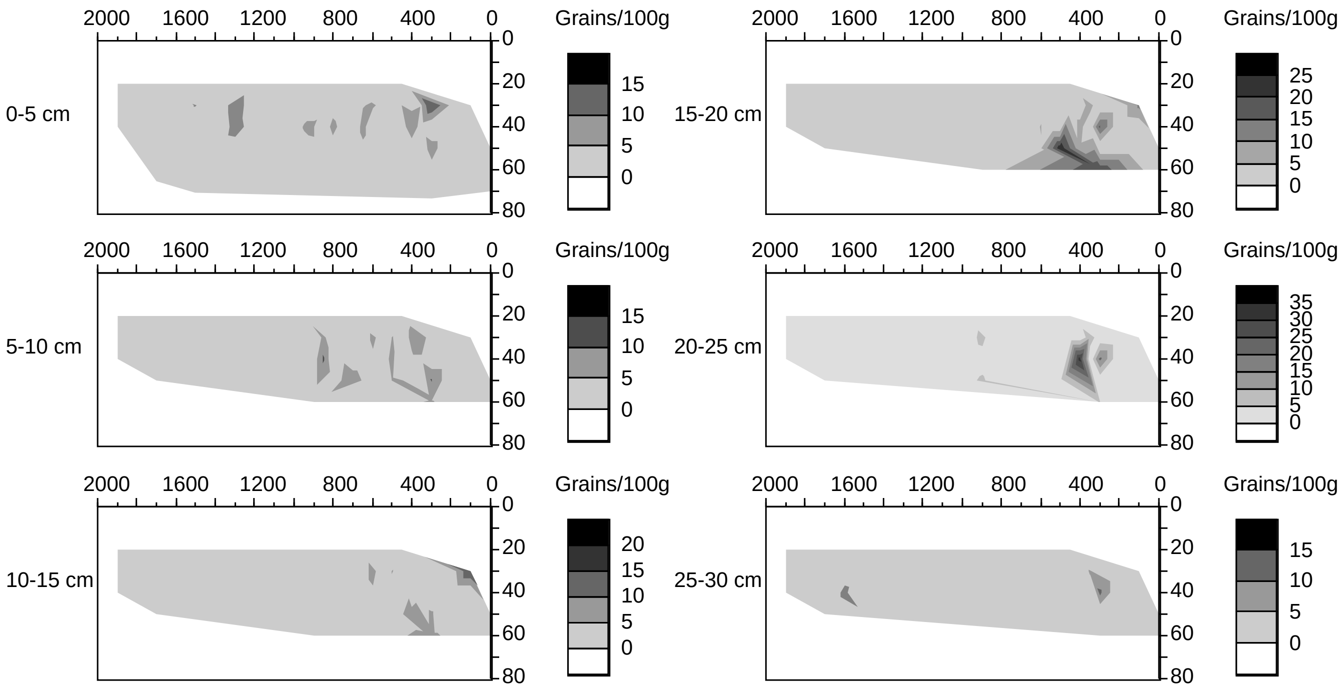

Fig. 5 Maps of distribution of tracers in the sampled area for each depth interval in the cores, expressed as number of grains for 100 g of sample. The horizontal axis represents the longshore distance (m) away from the injection point, the vertical axis represents the cross-shore distance (m) measured from a reference point located in the back-shore (see Fig. 2). The berm top is located at a cross-shore distance of 20 m away from the origin

Discussion

Previous studies found that the main variable controlling the depth of sand activation is the wave height. King (1951) concluded that the depth of disturbance was about 30% of the wave height, while Komar and Inman (1970) obtained a ratio of about 8%. Experiments in Japan (Kraus et al. 1982; Kraus 1985) lead to the formulation of an empirical relationship between mixing depth (Z_m) and significant wave height at breaking (H_{sb}):

$$Z_m = 0.027\ H_{sb} \tag{5}$$

The relationship given above was obtained on beaches with different morphodynamics and granulometry, most of them dissipative in a microtidal context, so that other authors found limitations in applying the formula when dealing with reflective beaches. Sherman et al. (1994) proposed a new relationship from data on low-energy reflective beaches:

$$Z_m = 0.22\ H_{sb} \tag{6}$$

Application of Eq. 6 to the wave data at Praia de Faro predicts an activation depth of 17.6 cm, 5.5 cm less than the average value observed in the field (23.1 cm), that supports a Z_m/H_{sb} ratio of 29%, similar to the one initially proposed by King (1951) and equal to the one obtained by a study on another reflective beach (Culatra Island) of the Ria Formosa (Ciavola et al. 1997a).

Kraus (1985) also proposed that the cross-shore distribution of mixing depth should have a first maximum at the wave breaking point and a second maximum in the swash. The mixing profile observed at Praia de Faro (Fig. 6) has instead a minimum in the swash, with a pattern that remained constant in all core lines (up to 1900 m away from the injection point), so that local effects can be excluded. A similar pattern was observed in other studies on reflective beaches (Sherman et al. 1994; Ciavola et al. 1997b), therefore the difference with Kraus (1985) is related to the fact he studied mainly dissipative beaches in a microtidal context.

In order to compare the experimental results on sand transport with the theoretical prediction, it is useful to transform volumetric rates into immersed weight rates (I_l) expressed in Newtons per second, using the formula proposed by Inman and Bagnold (1963):

$$I_l = (\rho_s - \rho)(1 - p)Q \tag{7}$$

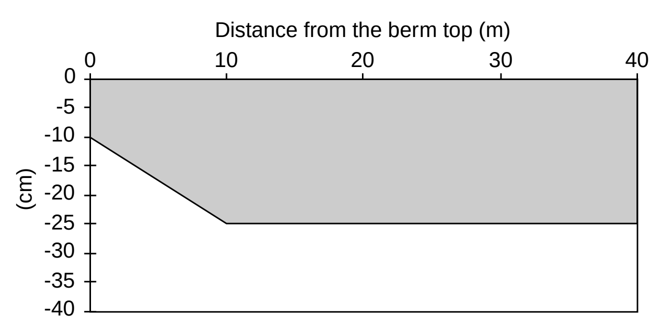

Fig. 6 Cross-shore profile of mixing depth

where ρ_s is the sand density, ρ the seawater density, p the sand porosity (0.4), and Q the volume of transported sand. Application of Eq. 7 to the Praia de Faro data gives a transport of about 1337 N s^{-1}. Equation 7 can be related to wave-driven forces causing longshore drift as (Komar and Inman 1970):

$$I_l = K\ P_l = K\ (ECn)_b \sin \alpha_b \cos \alpha_b \tag{8}$$

where E is the total wave energy ($1/8\rho g H^2$), Cn the wave group velocity calculated using linear wave theory ($\sqrt{g1.28H}$), α the angle between the wave front and the shoreline, and the subscript b refers to all conditions measured at breaking point. The only unknown term of Eq. 8 is the coefficient K, which was initially proposed to be 0.77 by Komar and Inman (1970), using in the computation of Eq. 8 the mean squared wave height H_{rms}, which, according to Komar (1988), corresponds to the correct parameter for the assessment of wave energy using complete spectra. If the K of Komar and Inman (1970) is used, the computed I_l is 307 N s^{-1}, equivalent to a volume rate of 0.032 m^3/s (2.8×10^3 m^3 day^{-1}), thus more than four times smaller than the observed transport.

As pointed out by Allen (1985), the wave group velocity in Eq. 8 is generally computed using Airy's wave theory for ease of calculation, even if it would be better to use solitary wave theory, which provides a more realistic description of nearshore conditions. According to solitary wave theory, the breaker velocity is equal to:

$$C = \sqrt{g(h + H)_b} \tag{9}$$

where h is the water depth below the still water level, and H is the wave height (in this case H_{rms}), both measured at break point. Note that the array of pressure sensors deployed at Praia de Faro measured, on average, a water depth at breaking of 1 m; therefore the breaker velocity is larger than that computed using linear wave theory. If this value of breaker velocity is used in Eq. 8, a better approximation of the transport measured in the field is obtained. With a value of I_l equal to 444 N s^{-1}, corresponding to a volumetric rate of 0.047 m^3 s^{-1} (4.0×10^3 m^3 day^{-1}), the calculated transport rate is three times smaller than the rate measured with the tracers.

If Eq. 8 is solved using the measured rate of immersed transport and the longshore energy flux computed using solitary wave theory, a K of 2.32 is obtained. The determined K is larger than the 0.58 previously proposed by Kraus et al. (1982) carrying out experiments in Japan, and than the 1.15 determined by Dean et al. (1982) at Santa Barbara in California, although work by Duane and James (1980) had already estimated values of K larger than 2.

Several authors have considered the influence of granulometry, beach slope, and wave parameters on longshore transport (e.g., Dean et al. 1982; Kamphuis 1991), but Komar (1988) concluded that existing data are insufficient to establish reliable empirical relationships, mainly because of the heterogeneity in methodologies of data collection, despite recognizing that an influence of environmental factors must exist. Other authors (Bodge and Kraus 1991) proposed an influence of wave directional spreading within the gravity band and surf beat on the determination of K. Furthermore, variability in predicted longshore transport rates can be due to the assumptions that sand density is 2650 kg m^{-3} (valid only for pure quartzitic sands) and that beach porosity is always 0.4 over the whole foreshore, while it is obviously influenced by the presence of pore water, sediment sorting, etc. These assumptions can cause an underestimation of transport of about 27% for low-density, well-sorted sands and overestimation of up to 19% for badly sorted heavy sands (Bodge and Kraus 1991). Other sources of uncertainty can be errors in wave estimation (Komar 1988) and the effect of large-scale bedforms (Sherman et al. 1993).

Finally, a significant limitation in the predictive capability of longshore transport models exists using the wave energy flux approach, that is, the dependency of transport on breaker type is considered (Beach and Sternberg 1996). As Bodge (1989) pointed out, after reviewing published data on longshore transport in the surf zone, plunging and collapsing breakers produce greater longshore transport than spilling breakers, for a given energy flux. Recently Beach and Sternberg (1996) substantiated this conclusion using a line of measuring arrays (OBS) at five positions across the surf zone. In this case, plunging waves were responsible for most of the suspended load, longshore, and cross-shore flux of sediment, while bores, spilling waves, and unbroken waves were less important. Therefore, the fact that waves at Faro Beach were mostly plunging breakers supports the relatively large transport compared to estimations using equations that do not include parameters to describe breaker type.

Direct measurements of longshore transport have been carried out with a variety of methodologies such as tracers, sediment traps, and remote sensors. Allen (1988) provides a succinct review of the methodologies, considering advantages and disadvantages of each one, arguing that small-scale experiments can provide a quantitative refinement needed to verify or improve knowledge in many areas of sediment transport research. There are, however, few comparative studies that can clearly identify the limitation of each methodology, providing a correction factor for a transport measurement with a method, to make it fully comparable with another estimate obtained in a different way.

Conclusions

The field experiment that was carried out at Praia de Faro employed simple field and laboratory techniques to determine experimental longshore transport rates. It is interesting to observe that the sand transport during the experiment was caused by waves approaching the beach from the SE at high angles (20°), causing strong longshore drift westwards in opposition to the regional pattern of transport.

Determination of sand mixing depths on the beach lead to a Z_m/H_{sb} ratio of 29%, in agreement with recent research on beaches in similar field conditions (reflective beaches under plunging waves). The cross-shore mixing profile had a maximum in the area of breakers and a minimum in the swash zone. Longshore transport was larger than theoretical calculations using bulk transport predictors, pointing out the limitations of transport models without proper calibration. Considering that most waves measured in the field were plunging breakers, the application of solitary wave theory seems to have provided a more realistic approximation of energy than linear wave theory.

This paper presents a detailed description of the fluorescent tracer methodology for quantifying sand transport, and it is hoped that more authors will revisit this technique. It offers the advantages of reproducibility, low cost, and low environmental impact. Most formulas for longshore transport were calibrated for low to medium wave energies and low-gradient beaches, so they often are used for conditions outside the calibration limits, especially for engineering studies, where time and financial constraints do not allow field experiments. More sedimentological studies of this kind should be carried out on beaches throughout the world, to improve the field database on longshore transport, since theoretical estimation still remains largely based on empirical tests.

Acknowledgments The field experiment LUAR-Faro '96 was carried out by the Grupo Disepla of the Universidade do Algarve with support from the HCM project "Coastal Environments (E-Atlantic): Physical Processes" of the European Union (ERBCHRX-CT-94-0541). We are grateful to all field participants from the universities of Algarve, Lisbon, Cadiz (Spain), and Vale do Itajaí (Brazil). The authorities of the Parque Natural da Ria Formosa and Capitania de Faro kindly gave permission to carry out the experiment. The Instituto Hidrográfico supplied offshore wave data. Special thanks to Dr. Oliveira Pires for providing wave forecasts of great help in planning the experiment and to Mr. Mike Wilkin for his valuable technical support. Lastly, the experiment could not have been carried out without the help of the owner of the Paquete Restaurant, who offered us a shelter when the weather was cold and wet. This paper is contribution no. A93 of the Grupo Disepla. Manuscript preparation was supported by the RIMAR (PRAXIS XXI 2/2 1/MAR1743/13) and SWAMIEE (FMRX-CT97-0111) projects.

References

Abecasis F, Matias MF, Reis de Carvalho JJ, and Vera-Cruz D (1962) Methods of determining sand and silt movement along the coast, in estuaries and in maritime rivers. Laboratório Nacional de Engenharia Civil Technical Paper no. 186. Lisbon: Ministério das Obras Públicas. 25 pp

Allen JR (1985) Field measurements of longshore sediment transport: Sandy Hook, New Jersey, USA. Journal Coastal Research 1 : 231–240

Allen JR (1988) Nearshore sediment transport. Geographical Review 78 : 148–157

Andrade C (1990) O ambiente de barreira da Ria Formosa, Algarve, Portugal. Unpublished PhD thesis. Lisbon: Department of Geology, University of Lisbon. 645 pp

Beach RA and Sternberg RW (1996) Suspended-sediment transport in the surf zone: response to breaking waves. Continental Shelf Research 16 : 1989–2003

Bettencourt P (1994) Les environments sedimentaires de la Côte Sotavento (Algarve, Sud Portugal) et leur évolution Holocène et actuelle. Unpublished PhD thesis. Bordeaux, France: Department of Geology and Oceanography, University of Bordeaux I. 2 volumes

Bodge KR (1989) A literature review of the distribution of longshore sediment transport across the surf zone. Journal Coastal Research 5 : 307–328

Bodge KR and Kraus NC (1991) Critical examination of longshore transport rate magnitude. Proceedings Coastal Sediments '91. New York: ASCE. pp 139–155

Chandramohan P, Nayak B, and Anand N (1994) Crest-breaking time-lapse approach for measuring breaker angle. Journal of Waterway, Port, Coastal and Ocean Engineering 120 : 318–324

Ciavola P, Taborda R, Ferreira Ó, and Alveirinho Dias J (1997a) Field measurements of longshore sand transport and control processes on a steep meso-tidal beach in Portugal. Journal of Coastal Research 13 : 1119–1129

Ciavola P, Taborda R, Ferreira Ó, and Alveirinho Dias J (1997b) Field observations of sand-mixing depths on steep beaches. Marine Geology 141 : 147–156

Dean RG, Berek EP, Gable CG, and Seymour RJ (1982) Longshore transport determined by an efficient trap. Proceedings 18th Coastal Engineering Conference. New York: ASCE. pp 954–968

Dias JMA (1986) Observações sobre a origem das areias das ilhas de barreira da Ria Formosa Proceedings 4th Congresso do Algarve. Faro, Portugal. pp 579–587

Downing JP, Sternberg RW, and Lister CRB (1981) New instrumentation for the investigation of sediment suspension processes in the shallow marine environment. Marine Geology 42 : 19–34

Duane DB and James WR (1980) Littoral transport in the surf zone elucidated by an eulerian sediment tracer experiment. Journal of Sedimentary Petrology 50 : 929–942

Greenwood B and Hale PB (1980) Depth of activity, sediment flux and morphological change in a barred nearshore environment. In: McCann SB (Ed.), The Coastline of Canada: Halifax, Canada, Geological Survey of Canada. pp 89–109

Guza RT and Inman DL (1975) Edge waves and beach cusps. Journal of Geophysical Research 80 : 2997–3012

Ingle JC (1966) The Movement of Beach Sand. Amsterdam: Elsevier Publishing. 221 pp

Inman DL and Bagnold RA (1963) Littoral Processes. In: Hill MN (Ed.), The Sea, Vol. 3. New York: Wiley-Interscience. pp 529–553

Instituto Hidrográfico and Laboratório Nacional de Engenharia Civil (1994) Wave climatology of the Portuguese coast. Final report of subproject A. Lisbon, Portugal: NATO PO-WAVES Project. 80 pp

Kamphuis JW (1991) Alongshore sediment transport rate. Journal of Waterway, Port, Coastal and Ocean Engineering 117 : 624–640

Kidson C and Carr AP (1971) Marking beach materials for tracing experiments. In: JA Steers (Ed.), Introduction to Coastline Development. Basingstoke, UK: Macmillan. pp 69–93

King CAM (1951) Depth of disturbance of sand on sea beaches by waves. Journal of Sedimentary Petrology 21 : 131–140

Komar PD (1988) Environmental controls on littoral sand transport. Proceedings 21st Coastal Engineering Conference. New York: ASCE. pp 1238–1252

Komar PD and Inman DL (1970) Longshore sand transport on beaches. Journal of Geophysical Research 75 : 5514–5527

Kraus NC (1985) Field experiments on vertical mixing of sand in the surf zone. Journal of Sedimentary Petrology 55 : 3–14

Kraus NC (1987) Application of portable traps for obtaining point measurements of sediment transport rates in the surf zone. Journal of Coastal Research 3 : 139–152

Kraus NC, Isobe M, Igarashi H, Sasaki TO, and Horikawa K (1982) Field experiments on longshore sand transport in the surf zone. Proceedings 18th Coastal Engineering Conference. New York: ASCE. pp 970–988

Madsen OS (1987) Use of tracers in sediment transport studies. Proceedings Coastal Sediments '87. New York: ASCE. pp 424–435

Pessanha LEV and Pires HNO (1981) Elementos sobre o clima de agitação marítima na costa sul do Algarve. Monografia de Meteorologia e Geofísica. Lisbon, Portugal: Instituto Nacional de Meteorologia e Geofisica. 67 pp

Pilkey OH Jr, Neal WJ, Monteiro JH, and Dias JMA (1989) Algarve barrier islands: a non coastal-plain system in Portugal. Journal of Coastal Research 5 : 239–261

Pinto JRC, Dias JMA, Fernandes SP, Ferreira Ó, Silva AV, and Taborda R (1994) Automatic system for tagged sand detection. Gaia 8 : 161–164

Pires H (1985) Alguns aspectos do clima de agitação marítima na costa sul do Algarve. Monografia de Meteorologia e Geofísica. Lisbon, Portugal: Instituto Nacional de Meteorologia e Geofísica. 30 pp

Richardson NM (1902) An experiment on the movements of a load of brickbats deposited on Chesil Beach. Proceedings, Dorset Natural History Field Club 23 : 123–133

Sherman DJ, Short AD, and Takeda I (1993) Sediment mixing-depths and megaripple migration in rip channels. Journal of Coastal Research Special Issue 15 : 39–48

Sherman DJ, Nordstrom KF, Jackson NL, and Allen JR (1994) Sediment mixing-depths on a low-energy reflective beach. Journal of Coastal Research 10 : 297–305

Taborda R, Ferreira Ó, Dias JMA, and Moita P (1994) Field observations of longshore sand transport in a high energy environment. In: de Carvalho S and Gomes V (Eds.), Proceedings of Littoral 94. Lisbon, Portugal: EUROCOAST. pp 479–487

Tomé Martins J, Ferreira Ó, Ciavola P, and Alveirinho Dias JMA (1996) Monitoring of profile changes at Praia de Faro, Algarve: a tool to predict and solve problems. In: Taussik J and Mitchell J (Eds.), Partnership in Coastal Zone Management. Cardigan, UK: Samara Publishing Limited. pp 615–622

Vincent CE, Hanes DM, and Bowen AJ (1991) Acoustic measurements of suspended sand on the shoreface and the control of concentration by bed roughness. Marine Geology 96 : 1–18

Yasso WE (1966) Formulation and use of fluorescent tracers coatings in sediment transport studies. Sedimentology 6 : 287–301

Zenkovitch VP (1960) Fluorescent substances as tracers for studying the movements of sand on the sea bed. The Dock and Harbour Authority XL : 280–283